Int. J. Electrochem. Sci., 14 **(2019)** 11349 – 11357, doi: 10.20964/2019.12.44

International Journal of ELECTROCHEMICAL SCIENCE
www.electrochemsci.org

The Study of a Phosphate Conversion Coating on Magnesium Alloy AZ91D: IV. Comparison of Electrochemical Behaviors in Borate Buffer and Sodium Chloride Solutions

Jun Yang[1], *Pei Zhang*[2], *Yong Zhou*[3,*], *Fuan Yan*[3]

[1]The College of Post and Telecommunication of WIT, Wuhan Institute of Technology, Wuhan 430073, China
[2]College of Chemistry and Food Science, Yulin Normal University, Yulin 537000, China
[3]Key Laboratory for Green Chemical Process of Ministry of Education, Wuhan Institute of Technology, Wuhan 430205, China
[*]E-mail: zhouyong@wit.edu.cn

Received: 5 July 2019/ *Accepted:* 24 September 2019 / *Published:* 29 October 2019

This paper involved a phosphate conversion coating on magnesium alloy AZ91D. The phosphated magnesium alloy (PMA) was obtained via the preparation of phosphate conversion coating (PCC) on the surface of uncoated magnesium alloy (UMA). The electrochemical behaviors of PMA and UMA in the borate buffer (H_3BO_4) solution and in the sodium chloride (NaCl) solution were characterized with the electrochemical techniques of potentiodynamic polarization and electrochemical impedance spectroscopy (EIS), and the results were also compared. Both in the H_3BO_4 solution and in the NaCl solution, the corrosion current density (i_{corr}) and the total impedance ($Z_{all\text{-}in}$) of PMA were respectively smaller and larger than those of UMA, indicating the protective performance of PCC. However, the deviations of electrochemical parameters in the H_3BO_4 solution were significantly lower than those in the NaCl solution, which was due to the relatively stable pH value of H_3BO_4 solution, confirming the rationality of borate buffer solutions for the electrochemical measurements concerning magnesium alloys.

Keywords: magnesium alloy AZ91D; phosphate conversion coating; electrochemical behavior; H_3BO_4 solution; NaCl solution

1. INTRODUCTION

Magnesium alloys, because of excellent comprehensive properties, are used widely in different fields involving production and living [1-3]. However, the current application and the future development of magnesium alloys are limited by their poor corrosion resistance mainly, which is derived from the high activity and negative standard potential of Mg element [4]. In order to strengthen corrosion resistance, the methods of surface treatment are usually performed to prepare a protective

layer on the surface of magnesium alloys [5]. As a kind of main surface protective layer, chemical conversion coating and its preparation technology show some unique advantages, such as low cost, easy operation and so on [6]. Further, the process of phosphate conversion coating (PCC) is the one of relatively mature and low-toxic technology in the field of chemical conversion coating [7].

The present studies involving PCC on the surface of magnesium alloys are mainly focused on the following two aspects: one is the preparation and characterization of PCC, and the other one is the evaluation of corrosion resistance between phosphated magnesium alloy (PMA) and uncoated magnesium alloy (UMA). On the latter, the electrochemical measurements in borate buffer solutions are usually carried out. Inoue et al. [8] studied the electrochemical behaviors of pure magnesium, UMA AZ31 and UMA AZ91E in borate buffer solutions with different pH values in detail. The authors reported that the corrosion rate of pure magnesium and its alloys was independent on the purity and content of alloyed elements but was significantly dependent on the pH value of tested solutions. Further, it is generally accepted that it is appropriate to conduct the electrochemical measurements of pure magnesium and its alloys in the borate buffer (H_3BO_4) solution with 0.93 g/L H_3BO_4 as well as 9.86 g/L $Na_2B_4O_7$ and at pH 9.2. The related reports are summarized as follows [9-12]. Li et al. [9] studied the electrochemical behaviors of PMA AZ91D and UMA AZ91D in the H_3BO_4 solution and reported that the UMA reacted acutely with the H_3BO_4 solution; compared with the UMA, the PMA showed relatively positive corrosion potential (E_{corr}), small corrosion current density (i_{corr}) and large polarization resistance (R_p), indicating that the corrosion resistance for the AZ91D alloy was strengthened when the PCC was prepared on the AZ91D surface. Yong et al. [10] studied the electrochemical behaviors of PMA AM60 and UMA AM60 in the H_3BO_4 solution. The authors reported that both the PMA and the UMA presented the electrochemical characteristic of active dissolution: in potentiodynamic polarization tests, the anodic current density increased gradually with the positive shift of applied potential; in electrochemical impedance spectroscopy (EIS) tests, the Nyquist plot was composed of two capacitive loops at high and low frequencies. Kouisni et al. [11] also studied the electrochemical behaviors of PMA AM60 and UMA AM60 in the H_3BO_4 solution and reported that the PCC slowed down the dissolution process of AM60 alloy considerably and provided considerable anti-corrosion protection to the AM60 alloy.

In our previous studies [13-15], a phosphating recipe and technology for the AZ91D alloy is obtained [13], and the coating-forming process and mechanism of PCC is also clarified and discussed [14]. However, the related electrochemical measurements in H_3BO_4 solutions are absent. At the same time, besides H_3BO_4 solutions, sodium chloride (NaCl) solutions are usually applied to evaluate the corrosion resistance of metals and alloys, particular 3.5 wt.% NaCl solution [16]. Nevertheless, the electrochemical measurements of PMA and UMA in NaCl solutions are relatively few. Therefore, in this work, the PMA AZ91D is obtained via the preparation of PCC on the surface of UMA AZ91D; after that, the electrochemical behaviors of PMA and UMA in the H_3BO_4 solution (0.93 g/L H_3BO_4, 9.86 g/L $Na_2B_4O_7$, pH 9.2) and in the NaCl solution (3.5 wt.%, pH 7) are characterized with the electrochemical techniques of potentiodynamic polarization and EIS, and the results are also compared and discussed in detail.

2. EXPERIMENTAL

2.1 Material

The studied material was magnesium alloy AZ91D with the following chemical composition: Al, 9.400; Zn, 0.8200; Mn, 0.2300; Si, 0.0100; Cu, 0.0200; Ni 0.0021; Fe, 0.0050, and Mg, balance. Samples were manually abraded up to 1000 grit with SiC abrasive papers, rinsed with deionized water and degreased in acetone.

2.2 PCC preparation

The phosphating recipe was composed of ZnO 2.0 g/L, H_3PO_4 12.0 g/L, NaF 1.0 g/L, $C_4H_4O_6Na_2$ 4.0 g/L, $NaNO_3$ 6.0 g/L and $Na_4P_2O_7$, 0.5 g/L. The phosphating temperature was 45 ℃, and the phosphating time was 20 min. Each UMA was suspended with PTFE and then was immersed in the phosphating bath to prepare PCC.

2.3 Electrochemical measurement

The electrochemical measurements of potentiodynamic polarization and EIS were carried out using a CS310 electrochemical workstation (China). The tested electrolytes were the H_3BO_4 solution with 0.93 g/L H_3BO_4 as well as 9.86 g/L $Na_2B_4O_7$ at pH 9.2 and the NaCl solution with 3.5 wt.% NaCl at pH 7. A typical three electrode system was used for the potentiodynamic polarization and EIS tests. The system was composed of a saturated calomel electrode (SCE) as reference electrode, a platinum sheet as counter electrode and the PMA or UMA as working electrode. Before each electrochemical test, the working electrode was immersed in the corresponding solution for a certain period of time until the open circuit potential (OCP) was stable. In the potentiodynamic polarization test, the potential scanning rate was 0.5 mV/s, and the potential scanning range was from -0.3 V_{OCP} to 0.3 V_{OCP}. In the EIS test, a perturbation potential of 10 mV amplitude was applied in the frequency range from 10^5 Hz to 10^{-2} Hz. The potentiodynamic polarization and EIS tests were performed at ambient temperature.

3. RESULTS AND DISCUSSION

3.1 Potentiodynamic polarization test

Fig. 1 shows the polarization curves of PMA and UMA in the H_3BO_4 solution and in the NaCl solution. From the polarization curves shown in Fig. 1, for the PMA and UMA in the two solutions, anodic current density increases significantly with the positive shift of applied potential, indicating that both PMA and UMA presented the electrochemical behavior of active dissolution in the H_3BO_4 and NaCl solutions [17].

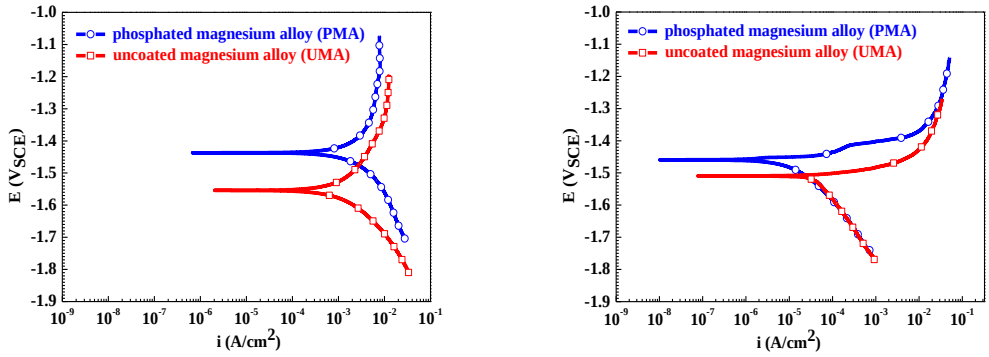

Figure 1. Polarization curves of PMA and UMA (a) in H_3BO_4 solution and (b) in NaCl solution.

In order to obtain the relatively accurate values of E_{corr} and i_{corr}, ten repetitions of potentiodynamic polarization test were carried out. After that, the Tafel interpretation was applied to analyze the potentiodynamic polarization results via the CVIEW software. Table 1 lists the mean values of E_{corr} and i_{corr} from the ten parallel potentiodynamic polarization tests. From Table 1, in the two solutions, the E_{corr} and i_{corr} values for the PMA are respectively higher and smaller than those for the UMA, confirming the protective performance of PCC.

Table 1. Mean values of E_{corr} and i_{corr} from ten parallel potentiodynamic polarization tests.

	E_{corr} (V_{SCE})		i_{corr} (mA/cm^2)	
	PMA	UMA	PMA	UMA
H_3BO_4 solution	-1.44	-1.55	-1.46	-1.51
NaCl solution	0.47	1.05	15.03	17.49

The effect of PCC presence on the variation of Ecorr and icorr is discussed as follows. For magnesium alloys in corrosion media, the main anodic reaction is the Mg oxidation:

$Mg \rightarrow Mg^{2+} + 2e$ (1)

In contrast, the cathodic reaction is relatively complicated: in strong acidic corrosion media, the dominated cathodic reaction is the H^+ reduction:

$2H^+ + 2e \rightarrow H_2$ (2)

In weak acidic and alkaline corrosion media, the dominated cathodic reaction is the O_2 reduction:

$O_2 + 2H_2O + 4e \rightarrow 4OH^-$ (3)

In this work, the pH values of H_3BO_4 solution and NaCl solution are pH 9.2 and pH 7.0, respectively. Therefore, the cathodic reaction of O_2 reduction becomes the main cathodic reaction. Further, it is confirmed that surface protective layers mainly provide a physical barrier to restrain the permeation of aggressive species from bulk solution to material surface and the diffusion of corrosion products from material surface to bulk solution [18]. Therefore, the PCC is present on the surface of

PMA: on the one hand, the equilibrium potential of Mg^{2+}/Mg moves to the positive direction, resulting in the positive shift of E_{corr}; on the other hand, the chemical equilibrium of Mg oxidation moves to the left direction, leading to the decrease of i_{corr}.

However, it is noteworthy that the obvious difference of E_{corr} and i_{corr} for the PMA and UMA in the H_3BO_4 solution and in the NaCl solution is present, which will be compared and discussed later.

3.2 EIS test

Fig. 2 shows the EIS of PMA and UMA in the H_3BO_4 solution and in the NaCl solution. From the EIS shown in Fig. 2a, for the PMA and UMA in the H_3BO_4 solution, the Nyquist plots are composed of two depressed capacitive semicircles at high and low frequencies. For the PMA, the semicircle at high frequency is attributed to the presence of PCC in the surface of PMA [7], and the other semicircle at low frequency is due to the charge transfer between double electron layer [19]. Besides, for the UMA, the semicircle at high frequency is derived from the presence of air-formed oxide film on the surface of UMA [10], and the other semicircle at low frequency is also due to the process of charge transfer. In contrast, the Nyquist plots of PMA and UMA in the NaCl solution are relatively complicated, as shown in Fig. 2b. On the one hand, the Nyquist plot of PMA in the NaCl solution is similar to that of PMA in the H_3BO_4 solution: two depressed capacitive semicircles are present on the Nyquist plot. On the other hand, the Nyquist plot of UMA is composed of a capacitive semicircle at high frequency and an inductive semicircle at low frequency: the capacitive semicircle is attributed to the charge transfer between double electron layer, and the inductive semicircle is due to the adsorption of aggressive anions, mainly Cl^-, on the surface of UMA [20].

Although the significantly different EIS characteristic of PMA and UMA in the H_3BO_4 solution and in the NaCl solution, the total impedance ($Z_{all\text{-}in}$) for the PMA is obviously greater than that for the UMA, also confirming the protective performance of PCC.

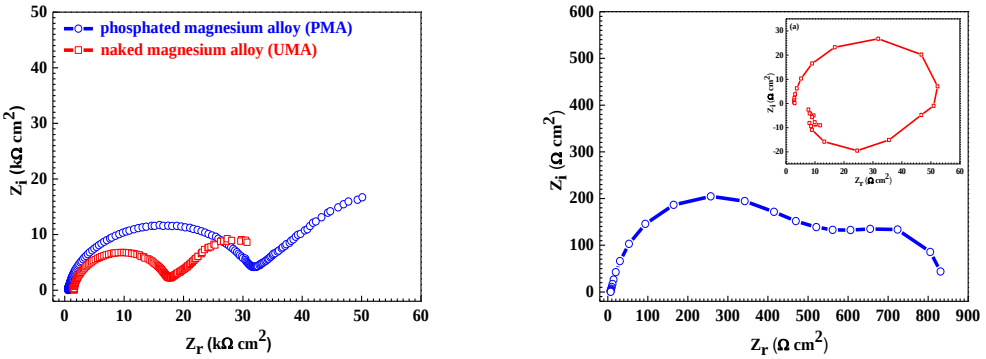

(a) (b)

Figure 2. EIS of PMA and UMA (a) in H_3BO_4 solution and (b) in NaCl solution.

At the same time, the equivalent electrical circuit (EEC) interpretation was applied to analyze the EIS results via the ZVIEW software. For the PMA in the H_3BO_4 solution and in the NaCl solution as well as for the UMA in the NaCl solution, the three Nyquist plots are composed of two depressed capacitive semicircles, so the EEC model shown in Fig. 3a is appropriate to analyze the corresponding

EIS [21]. In Fig. 3a, R_S represents the solution resistance, CPE_C and R_C respectively represent the PCC capacitance and resistance, CPE_f and R_f respectively represent the capacitance and resistance of air-formed oxide film, CPE_{dl} represents the double electron layer capacitance and R_{ct} represents the charge transfer resistance. At the same time, for the UMA in the NaCl solution, the Nyquist plot is composed of a capacitive semicircle and an inductive semicircle, so the EEC model shown in Fig. 3b is rational [22], where R_L represents the inductive resistance and L represents the pure inductance.

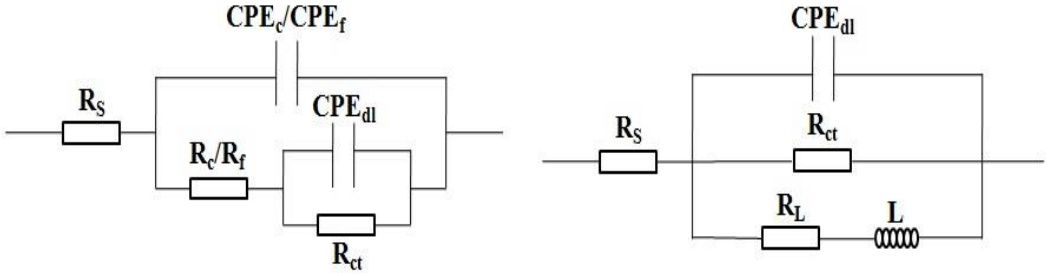

(a) (b)

Figure 3. EEC models for EIS analysis.

In order to obtain the relatively accurate values of R_C and R_{ct}, ten repetitions of EIS test were carried out. Table 2 lists the mean values of R_C and R_{ct} from the ten parallel EIS tests. From Table 2, in the two solutions, the R_{ct} value for the PMA is larger than that for the UMA, confirming the protective performance of PCC.

Table 2. Mean values of R_C and R_{ct} from ten parallel EIS tests.

	R_C (kΩ cm^2)		R_{ct} (kΩ cm^2)	
	PMA	UMA	PMA	UMA
H_3BO_4 solution	32.16	/	17.52	13.39
NaCl solution	0.61	/	0.67	0.52

3.3 Analysis and comparison

Fig. 4 shows the means and the deviations of E_{corr}, i_{corr}, R_C and R_{ct} for the PMA and UMA in the H_3BO_4 solution and in the NaCl solution. As shown in Fig. 4b and Fig. 4d, in the two solutions, the i_{corr} and R_{ct} values for the PMA are respectively smaller and larger than the corresponding values for the UMA, further confirming the protective performance of PCC. On the other hand, for the PMA and UMA, the i_{corr} values in the H_3BO_4 solution is smaller than those in the NaCl solution shown in Fig. 4b, the R_C value in the H_3BO_4 solution is larger than that in the NaCl solution shown in Fig. 4c, and the R_{ct} values in the H_3BO_4 solution are also larger than those in the NaCl solution shown in Fig. 4d, which is due to the different inhibitive/aggressive characteristics of H_3BO_4 solution and NaCl solution.

In corrosion environments, the inhibition of BO_4^{3-} and the aggression of Cl^- for the metals and alloys have been reported repeatedly [23-26].

However, it is worth noting from Fig. 4 that the deviations of E_{corr}, i_{corr}, R_C and R_{ct} in the H_3BO_4 solution are significantly lower than those in the NaCl solution, suggesting the rationality of H_3BO_4 solution for the electrochemical measurements on the PMA and UMA. Many studies have been carried out to select an appropriate electrolyte for the electrochemical measurements concerning phosphated metals and alloys [27-30], including 5.0 wt.% NaCl solution [27], 0.005 M Na_2HPO_4 solution [28], 0.1 M H_2SO_4 solution [29], 0.5 M NaCl solution [29] and 0.1 M NaOH solution [29]. Although the electrolytes containing Cl^- are usually used to evaluate the corrosion resistance of metals and alloys [31-33]; however, the stable pH value of tested electrolytes is crucial to the electrochemical tests on uncoated and phosphated magnesium alloys. Further, Kouisni et al. [11,34], Makara et al. [35], Gulbrandsen et al. [36] and Rudd et al. [37] reported that it is appropriate for the borate buffer solutions to be used to perform the corrosion electrochemical studies on magnesium alloys, particularly for the borate buffer solution containing 0.93 g/L H_3BO_4 and 9.86 g/L $Na_2B_4O_7$ at pH 9.2.

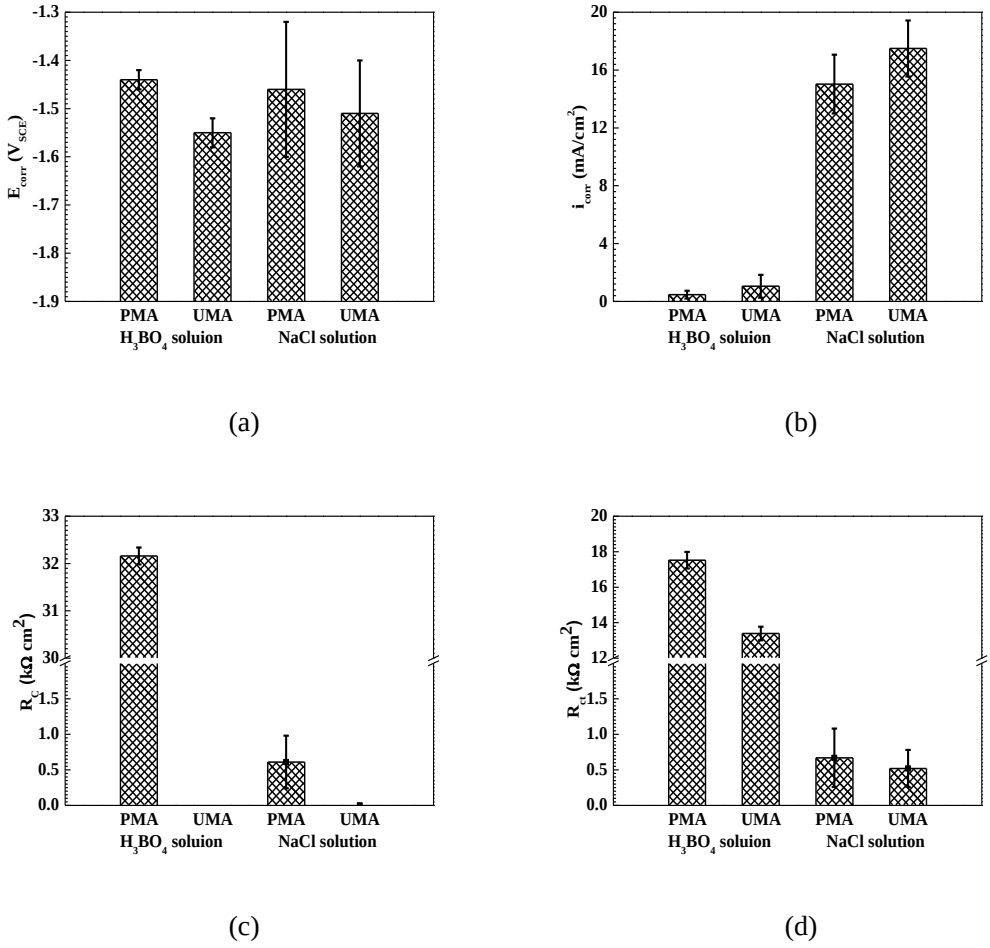

Figure 4. Means and deviations of E_{corr}, i_{corr}, R_C and R_{ct} for PMA and UMA in H_3BO_4 solution and in NaCl solution.

4. CONCLUSIONS

The electrochemical behaviors of PMA and UMA in the H_3BO_4 and NaCl solutions were characterized, and the PCC provided a certain anti-corrosion protection to the AZ91D alloy. The deviations of E_{corr}, i_{corr}, R_C and R_{ct} for the PMA and UNA in the H_3BO_4 solution was significantly lower than those in the NaCl solution, and the relatively stable pH value played a critical role in the availability of H_3BO_4 solution for the electrochemical measurements on the uncoated and phosphated magnesium alloys.

References

1. W.M. Jiang, X. Chen, B.J. Wang, Z.T. Fan and H.B. Wu, *International Journal of Advanced Manufacturing Technology*, 83 (2016) 167.
2. Z.S. Gao, S.L. Xie, B. Zhang, X.H. Qiu and F.X. Chen, *Chemical Engineering Journal*, 319 (2017) 108.
3. S. Ilyas, R.A. Chi and J.C. Lee, *Mineral Processing and Extractive Metallurgy Review*, 34 (2013) 185.
4. M. Liu, L. Wu, F.Q. Zhang and J. Fu, *Friction*, 4 (2016) 116.
5. F.G. Deng, L.S. Wang, Y. Zhou, X.H. Gong, X.P. Zhao, T. Hu and C.G. Wu, *RSC Advance*, 7 (2017) 48876.
6. Y. Luo, J.Q. Zhou, X. Yang and R. Liu, *Microgravity Science and Technology*, 30 (2018) 165.
7. Y. Zhou, J.P. Xiong and F.A. Yan, *Surface and Coatings Technology*, 328 (2017) 335.
8. H. Inoue, K. Sugahara, A. Yamamoto and H. Tsubakino, *Corrosion Science*, 44 (2002) 603.
9. Q. Li, S.Q. Xu, J.Y. Hu, S.Y. Zhang, X.K. Zhong and X.K. Yang, *Electrochimica Acta*, 55 (2010) 887.
10. Z.Y. Yong, J. Zhu, C. Qiu and Y.L. Liu, *Applied Surface Science*, 255 (2008) 1672.
11. L. Kouisni, M. Azzi, F. Dalard and S. Maximovitch, *Surface and Coatings Technology*, 192 (2005) 239.
12. P. Zhong, K.F. Ping, X.H. Qiu and F.X. Chen, *Desalination and Water Treatment*, 93 (2017) 109.
13. Q.Y. Xiong, Y. Zhou and J.P. Xiong, *International Journal of Electrochemical Science*, 10 (2015) 8454.
14. Y. Zhou, Q.Y. Xiong and J.P. Xiong, *International Journal of Electrochemical Science*, 10 (2015) 2812.
15. Q.Y. Xiong, J.P. Xiong, Y. Zhou and F.A. Yan, *International Journal of Electrochemical Science*, 12 (2017) 4238.
16. H.L. Huang and J. Tian, *Microelectronics Reliability*, 78 (2017) 131.
17. Y. Zhou and F.A. Yan, *International Journal of Electrochemical Science*, 11 (2016) 3976.
18. J. Li, C.Y. Xiong, J. Li, D. Yan, J. Pu, B. Chi and L. Jian, *International Journal of Hydrogen Energy*, 42 (2017) 16752.
19. X. Chen, Q.Y. Xiong, F. Zhu, H. Li, D. Liu, J.P. Xiong and Y. Zhou, *International Journal of Electrochemical Science*, 13 (2018) 1656.
20. A.M. Fefry and M.Z. Fatayerji, *Electrochimica Acta*, 54 (2009) 6522.
21. Y. Zhou, H.J. Huang, P. Zhang, D. Liu and F.A. Yan, *Surface Review and Letters*, 26 (2019) No. 1850218.
22. D. Liu, Y.Y. Li, Y. Zhou and Y.D. Ding, *Materials*, 11 (2018) No. 908.
23. E. Fujioka, H. Nishihara and K. Aramaki, *Corrosion Science*, 38 (1996) 1915.
24. L.C. Chen, P. Zhang, Q.Y. Xiong, P. Zhao, J.P. Xiong, Y. Zhou, *International Journal of Electrochemical Science*, 14 (2019) 919.

25. X.H. Qiu and W. Wang, *Journal of water process engineering*, 17 (2017) 271.
26. Y. Zhou, P. Zhang, J.P. Xiong and F.A. Yan, *RSC Advance*, 9 (2019) 23589-23597.
27. K. Kiss and M.C. Palagod, *Corrosion*, 43 (1987) 8.
28. J. Flis, Y. Tobiyama, K. Mochizuki and C. Shiga, *Corrosion Science*, 39 (1997) 1757.
29. D. Wang, P. Jokiel, A. Uebleis and H. Boehni, *Surface and Coatings Technology*, 88 (1996) 147.
30. Y. Zhou, P. Zhang, Y. Zuo, D. Liu and F.A. Yan, *Journal of the Brazilian Chemical Society*, 28 (2017) 2490.
31. X.G. Feng, X.Y. Lu, Y. Zuo, N. Zhuang and D. Chen, *Corrosion Science*, 103 (2016) 223-229.
32. H.L. Huang, Z.Q. Pan, Y.B. Qiu and X.P. Guo, *Microelectronics Reliability*, 53 (2013) 1149.
33. Y. Zhou, P. Zhang, H.J. Huang, J.P. Xiong, F.A. Yan, *Journal of the Brazilian Chemical Society*, 30 (2019) 1688.
34. L. Kouisni, M. Azzi, M. Zertoubi, F. Dalard and S. Maximovitch, *Surface and Coatings Technology*, 185 (2004) 58.
35. G.L. Makar and J. Kruger, *Journal of the Electrochemical Society*, 137 (1990) 414.
36. E. Gulbrandsen, *Electrochimica Acta*, 37 (1992) 1403.
37. A.L. Rudd, C.B. Berslin and F. Mansfeld, *Corrosion Science*, 42 (2000) 275.

© 2019 The Authors. Published by ESG (www.electrochemsci.org). This article is an open access article distributed under the terms and conditions of the Creative Commons Attribution license (http://creativecommons.org/licenses/by/4.0/).